Int. J. Adv. Appl. Math. and Mech. 5(4) (2018) 20 – 29 (ISSN: 2347-2529)

Journal homepage: www.ijaamm.com

IJAAMM

International Journal of Advances in Applied Mathematics and Mechanics

Entropy generation in a variable viscosity transient generalized Couette flow of nanofluids with Navier slip and convective cooling

Research Article

M. H. Mkwizu *, **A. X. Matofali**, **N. Ainea**

Department of Mathematics, Informatics and Computational Sciences, Solomon MahlanguCollege of Science and Education, Sokoine University of Agriculture, Morogoro-Tanzania

Received 04 January 2018; accepted (in revised version) 03 April 2018

Abstract: This work investigates the combined effects of thermophoresis, Brownian motion and variable viscosity on entropy generation in a transient generalized Couette flow of nanofluids with Navier slip and convective coolingof water-based nanofluids containing Copper (Cu) and Alumina (Al_2O_3) as nanoparticles. Both first and second laws of thermodynamics are applied to analyse the problem. The nonlinear governing equations of continuity, momentum, energy and nanoparticles concentration are tackled numerically using a semi discretization finite difference method together with Runge-Kutta Fehlberg integration scheme. Numerical results for velocity, temperature, and nanoparticles concentration profiles are obtained and utilised to compute the entropy generation rate, irreversibility ratio and Bejan number. Pertinent results are displayed graphically and discussed quantitatively.

Keywords: Nanofluids • Variable viscosity • Entropy generation • Bejan number • Thermophoresis • Brownian motion

1. Introduction

Nanotechnology has been widely used in engineering and industry since nanometer size materials possess unique physical and chemical properties. The addition of nanoscale particles into the conventional fluids like water, engine oil, ethylene glycol, etc., is known as nanofluid and was firstly introduced by Cho [1].

The model for a nanaofluid including the effects of Brownian motion and thermophoresis, introduced by Buongiorno [2] was applied by Kuznetsov and Nield [3] to the classical problem studied by Kuiken [4, 5] and Bejan [6] (Schmidt and Beckmann [6] , Kuiken, Bejan [7]), namely convective boundary layer flow past a vertical plate. In their pioneering paper Kuznetsov and Nield employed boundary conditions on the nanoparticle fraction analogous to those on the temperature. In this note the problem is revisited and a boundary condition that is more realistic physically is applied. It is no longer assumed that one can control the value of the nanoparticle fraction at the wall, but rather that the nanoparticle fluxes at the wall is zero. This change necessitates a rescaling of the parameters that are involved.

Mahdy and ChamkhaA [8] did a research on heat transfer and fluid flow of a non-Newtonian nanofluid over an unsteady contracting cylinder employing Buongiorno's model and found that the fluid velocity decreases initially due to the increase in the unsteadiness parameter; whereas the temperature and the concentration increase significantly in this case. The effect of increasing values of the Casson parameter is found to suppress the velocity field (in absolute sense), the temperature and concentration decrease as the Casson parameter increases. Both of dimensionless

* Corresponding author.
E-mail address(es): mkwizumh@gmail.com (M. H. Mkwizu).

temperatureand dimensionless concentration (in absolute sense) decrease with the increase of the unsteadiness parameters and the Brownian motion parameter. In addition, dimensionless temperature and dimensionless concentration (in absolute sense) increase as the Casson parameter and the thermophoresis parameter increase. The Prandtl number can be used to increase the rate of cooling in conducting flows. Mkwizu and Makinde [9] did a research on entropy generation in a variable viscosity channel flow of nanofluids with convective cooling. Results revealed that, general increase in entropy production across the channel with increasing viscous heating, pressure gradient and a decrease in nanofluid viscosity. The entropy generation and natural convection in a square cavity with a vertical heat source which is filled with copperâĂŞwater nanofluid was studied by Shahi et al. [10]. They found that the entropy generation decreases with the solid volume fraction.

Alam et al. [11] did a study on Convective flow of nanofluid along a permeable stretching/shrinking wedge with second order slip using BuongiornoâĂŹs mathematicalmodel. The results revealed that, base fluids and nanoparticles play an important role in heat transfer. Also addition of nanoparticles to the base fluid may not always increase the rate of heat transfer. It significantly depends on the surface convection and type of base fluid. Suction stabilizes the growth of the boundary layer. Velocity profiles within the boundary layer increase with the increase of the wedge angle parameter, unsteadiness parameter, shrinking parameter and second order slip parameter whereas it decrease with the increase values of the stretching parameter, Lewis number, thermophoresis parameter and first order slip parameter. Temperature within the boundary layer decreases with the increase of the wedge angle parameter, unsteadiness parameter and second order slip parameter while it increases with the increasing values of the Lewis number, Brownian motion parameter, thermophoresis parameter, first order slip parameter and Biot number (or surface convection parameter). Nanoparticle volume fraction within the boundary layer decreaseswith the increasing values of the wedge angle parameter, unsteadiness parameter, Lewis number ,Brownian motion parameter and second order slip parameter while it increases with the increasing values of the thermophoresis parameter, first order slip parameter andBiot number (or surface convection parameter).

The buoyancy effects on stagnation point flow and heat transfer of a nanofluid past a convectively heated stretching/shrinking sheet with or without magnetic field were considered by Makinde et al. [12] and Makinde [13]. Wang and Mujumdar [14] presented a comprehensive review of heat transfer characteristics of nanofluids.

Moakher et al. [15] did a research on new analytical solution of MHD fluid flow of fourth grade fluid through the channel with slip condition via collocation method.Theyconcluded that increasing the magnetic parameter leads to decrease in velocity values in whole domain. In addition,increasing in slip parameter caused a decrease in velocity components too.

Makinde et al. [16] performed numerous investigations to calculate entropy production and irreversibility due to flow and heat transfer of nanofluids over a moving flat surface. They found that the entropy generation in the flow system can be minimized by appropriate combination of parameter values together with nanoparticles volume fraction.

A numerical investigation of the effect of curvature and Reynolds number to radial velocity in a curved porous pipe was studied by Mwangiet al. [17]. They found that increase in curvature ratio leads to increase in radial velocity in the main pipe. Variation of curvature has negligible effect on the radial velocity through the porous wall. Also an increase in Reynolds number in the porous media leads to increase in radial velocity across the wall of the porous pipe for the same initial condition at the inner pipe wall.

In this study, we analyse the combined effects of thermophoresis, Brownian motion and variable viscosity on entropy generation rate intransient generalized Couette flow of nanofluids with Navier slip and convective coolingof water base nanofluid under the influence of convective heat exchange with the ambient surrounding. In the following sections the problem is formulated, numerically analysed and solved. Pertinent results are displayed graphically and discussed.

2. Mathematical model

Consider unsteady Couette flow of viscous incompressible nanofluids containing Copper (Cu) and Alumina (Al_2O_3) as nanoparticles. It is assumed that the upper wall moves with uniform velocity U at time $t > 0$ and exchange heat with the ambient surrounding following the Newton's law of cooling and the channel width is awith Navier slip at the bottomwall as depicted in Fig. 1 below. Using the Buongiorno nanofluid model with the Brownian motion, thermophoresis and nanoparticle volume fraction distributions, the governing equations for momentum, energy and nanoparticle concentration are

$$\rho_f \frac{\partial u}{\partial \bar{t}} = -\frac{\partial P}{\partial x} + \frac{\partial}{\partial y}\left(\mu_f(T)\frac{\partial u}{\partial y}\right) \tag{1}$$

$$\frac{\partial T}{\partial \bar{t}} = \alpha_f \frac{\partial^2 T}{\partial y^2} + \tau\left\{D_B \frac{\partial T}{\partial y}\frac{\partial C}{\partial y} + \frac{D_T}{T_a}\left(\frac{\partial T}{\partial y}\right)^2\right\} + \frac{\alpha_f \mu_f(T)}{k_f}\left(\frac{\partial u}{\partial y}\right)^2 \tag{2}$$

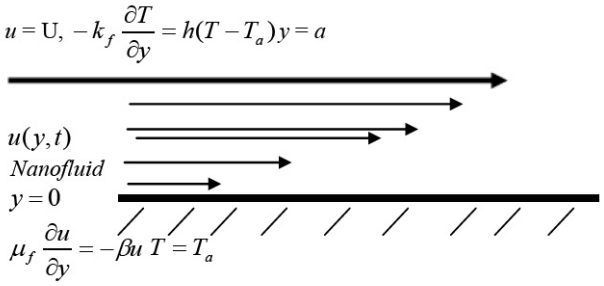

Fig. 1.

$$\frac{\partial C}{\partial \bar{t}} = D_B \frac{\partial^2 C}{\partial y^2} + \left(\frac{D_T}{T_a}\right)\left(\frac{\partial^2 T}{\partial y^2}\right) \tag{3}$$

where D_B and D_T are the Brownian and thermophoretic diffusion coefficients respectively,uis the nanofluid velocity in the x-direction, T is the temperature of the nanofluid, P is the nanofluid pressure, is the time, T_a is the ambient temperature which also correspond to the nanofluid initial temperature, is the concentration of nanoparticles, ρ_f is the density of the nanofluid, μ_f is the viscosity of the fluid fraction, α_f is the thermal diffusivity of the nanofluid, k_f is the thermal conductivity of the fluid fraction and τ is the ratio of solid particles heat capacitance to that of the nanofluid heat capacitance. The dynamic viscosity of nanofluid is assumed to be temperature dependent as follows:

$$\mu_f(T) = \mu_0 e^{-m(T-T_a)} \tag{4}$$

where Îij$_0$ is the nanofluid viscosity at the ambient temperature T_a, is a viscosity variation parameter which depends on the particular fluid. The initial and boundary conditions are given as follows:

$$u(y,0) = 0,\ \ T(y,0) = T_a,\ \mathrm{C}(y,0) = C_0, \mathbb{R} \tag{5}$$

$$\mu_f \frac{\partial u}{\partial y}\left(0,\bar{t}\right) = -\beta u\left(0,\bar{t}\right),\ \ T\left(0,\bar{t}\right) = T_w,\ \ C(0,\bar{t}) = C_w \tag{6}$$

$$u(a,\bar{t}) = U, -k_f \frac{\partial T}{\partial y}(a,\bar{t}) = h(T(a,\bar{t}) - T_a),\ D_B \frac{\partial C}{\partial y}(a,\bar{t}) = -\frac{D_T}{T_a}\frac{\partial T}{\partial y}(a,\bar{t}), \tag{7}$$

where h is the heat transfer coefficient and C_0 is the nanoparticles initial concentration. We introduce the non dimensionless variables and parameters as follows:

$$\left.\begin{aligned}
&\theta = \frac{T - T_a}{T_a},\quad W = \frac{ua}{v_f},\quad \eta = \frac{y}{a},\quad t = \frac{\bar{t} v_f}{a^2},\quad v_f = \frac{\mu_0}{\rho_f},\quad Bi = \frac{ha}{k_f},\\
&\overline{P} = \frac{a^2 P}{\mu_0^2},\quad Nb = \frac{\tau D_B C_0}{\alpha_f},\quad A = -\frac{\partial \overline{P}}{\partial X},\quad X = \frac{x}{a},\quad Pr = \frac{\mu_0 c_{pf}}{k_f},\quad Sc = \frac{v_f}{D_B},\\
&Ec = \frac{v_f^2}{c_{Pf} T_a a^2},\quad H = \frac{C}{C_0},\quad Nt = \frac{\tau D_T}{\alpha_f},\quad \tau = \frac{(\rho c_p)_s}{(\rho c_p)_f},\quad \beta = mT_a,\quad f = \frac{\mu_f}{\beta a}
\end{aligned}\right\} \tag{8}$$

The dimensionless governing equations together with the appropriate initial and boundary conditions can be written as:

$$\frac{\partial W}{\partial t} = A + e^{-\beta\theta}\frac{\partial^2 W}{\partial \eta^2} - \beta e^{-\beta\theta}\frac{\partial \theta}{\partial \eta}\frac{\partial W}{\partial \eta} \tag{9}$$

$$Pr\frac{\partial \theta}{\partial t} = \frac{\partial^2 \theta}{\partial \eta^2} + \left\{Nb\frac{\partial \theta}{\partial \eta}\frac{\partial H}{\partial \eta} + Nt\left(\frac{\partial \theta}{\partial \eta}\right)^2\right\} + EcPre^{-\beta\theta}\left(\frac{\partial W}{\partial \eta}\right)^2 \tag{10}$$

$$Sc\frac{\partial H}{\partial t} = \frac{\partial^2 H}{\partial \eta^2} + \frac{Nt}{Nb}\frac{\partial^2 \theta}{\partial \eta^2} \tag{11}$$

with

$$W(\eta,0)=0,\quad \theta(\eta,0)=0,\ H(\eta,0)=1, \tag{12}$$

$$\frac{\partial W}{\partial \eta}(0,t)=-\frac{\beta a}{\mu_f}W(0.t)\ ,\ \theta(0,t)=0,\ H(0,t)=0 \tag{13}$$

$$W(1,t)=1,\ \frac{\partial \theta}{\partial \eta}(1,t)=-Bi\theta(1,t), \tag{14}$$

$$\frac{\partial H}{\partial \eta}(1,t)=-\frac{Nt}{Nb}\frac{\partial \theta}{\partial \eta}(1,t), \tag{15}$$

where Nb is the Brownian motion parameter, Bi is the Biot number, Nt is the thermophoresis parameter, Sc is the Schmidt number, Pr is the Prandtl number, Ec is the Eckert number and A is the pressure gradient parameter.

The quantities of practical interest in this study are the skin friction coefficient C_f and the local Nusselt number Nu which are defined as

$$C_f=\frac{a^2\tau_w}{\rho_f v_f^2},\ Nu=\frac{aq_w}{k_f T_a}, \tag{16}$$

where τ_w is the wall shear stress and $q-w$ is the heat flux at the channel walls given by

$$\tau_w=\mu_f\left.\frac{\partial u}{\partial y}\right|_{y=a},\ q_w=-k_f\left.\frac{\partial T}{\partial y}\right|_{y=a} \tag{17}$$

Substituting Eq. (17) into (16), we obtain

$$\left.\begin{aligned} C_f&=e^{-\beta\theta}\frac{\partial W}{\partial \eta}\\ Nu&=-\frac{\partial \theta}{\partial \eta}\end{aligned}\right\}\quad \text{at}\quad \eta=1. \tag{18}$$

3. Entropy analysis

In the nanofluids flows, the improvement of the heat transfer properties causes the reduction in entropy generation. However, convection process involving channel flow of nanofluids is inherently irreversible. The non-equilibrium conditions due to the exchange of energy and momentum, within the nanofluid and at solid boundaries, cause continuous entropy generation. One part of this entropy production results from heat transfer in the direction of finite temperature gradients, while other part arises due to the fluid friction, nanoparticle concentration and complex interaction between the base fluid and the nanoparticles. The local volumetric rate of entropy generation is given by

$$S'''=\frac{k_f}{T_a^2}\left(\frac{\partial T}{\partial y}\right)^2+\frac{\mu_f(T)}{T_a}\left(\frac{\partial u}{\partial y}\right)^2+\frac{D_B}{C_0}\left(\frac{\partial C}{\partial y}\right)^2+\frac{D_B}{T_a}\frac{\partial T}{\partial y}\frac{\partial C}{\partial y} \tag{19}$$

The first term in Eq. (19) is the irreversibility due to heat transfer; the second term is the entropy generation due to viscous dissipation, while the third and the fourth terms are the local entropy generation due to nanoparticles mass transfer and complex interaction with the base fluid. Using Eq. (9), we express the entropy generation number in dimensionless form as,

$$Ns=\frac{a^2S'''}{k_f}=\left(\frac{\partial \theta}{\partial \eta}\right)^2+Bre^{-\beta\theta}\left(\frac{\partial W}{\partial \eta}\right)^2+\lambda\left[\left(\frac{\partial H}{\partial \eta}\right)^2+\frac{\partial H}{\partial \eta}\frac{\partial \theta}{\partial \eta}\right] \tag{20}$$

where $Br=EcPr$ is the Brinkmann number, $\lambda=\phi_0 D_B/k_f$ is the nanoparticles mass transfer parameter. Let

$$N_1=\left(\frac{\partial \theta}{\partial \eta}\right)^2,\quad N_2=Bre^{-\beta\theta}\left(\frac{\partial W}{\partial \eta}\right)^2\quad N_3=\lambda\left[\left(\frac{\partial H}{\partial \eta}\right)^2+\frac{\partial H}{\partial \eta}\frac{\partial \theta}{\partial \eta}\right] \tag{21}$$

The irreversibility distribution ratio is define as $\Phi=N_2/(N_1+N_3)$. Heat and nanoparticles mass transfer irreversibility dominates for $0\le\phi<1$ and fluid friction irreversibility dominates when $\Phi>1$. The contribution of both irreversibilities to entropy generation are equal when $\Phi=1$. We define the Bejan numbers (Be) mathematically as

$$Be=\frac{N_1+N_3}{Ns}=\frac{1}{1+\Phi}. \tag{22}$$

From Eq. (22), it is very obvious that the Bejan number ranges from 0 to 1. The zero value of the Bejan number corresponds to the limit where the irreversibility is dominated by the effect of fluid friction while $Be=1$ is the limit where the irreversibility due to heat and nanoparticles mass transfer dominates the flow system. Heat and mass transfer together with fluid friction irreversibilities are the same when the Bejan number equals 0.5.

4. Numerical procedure

Eqs. (10)-(15) constitute a system of nonlinear initial boundary value problem (IBVP) and are solved numerically using a semi-discretization finite difference method known as method of lines. A partition of the spatial interval $0 \leqslant \eta \leqslant 1$ into N equal parts is introduced such that the grid size $\Delta\eta = 1/N$ and grid points $\Delta\eta = 1/N$, $\Delta\eta = 1/N$. The semi-discretization finite difference technique known as method of line is employed to tackle the model nonlinear initial boundary value problem in (10)-(15). The discretization is based on a linear Cartesian mesh and uniform grid on which finite-differences are taken. The first and second spatial derivatives in Eqs. (10)-(12) are approximated with second-order central finite differences. Let $Wi(t)$,ïĄśi(t) and $Hi(t)$ be approximation of $W(\eta_i, t)$,$\theta(\eta_i, t)$ and $H(\eta_i, t)$, then the semi-discrete system for the problem becomes

$$\frac{dW_i}{dt} = A + e^{-\beta\theta_i}\frac{(W_{i+1} - 2W_i + W_{i-1})}{(\Delta\eta)^2} - \beta e^{-\beta\theta_i}\frac{(\theta_{i+1} - \theta_{i-1})(W_{i+1} - W_{i-1})}{4(\Delta\eta)^2}, \tag{23}$$

$$Pr\frac{d\theta_i}{dt} = \frac{(\theta_{i+1} - 2\theta_i + \theta_{i-1})}{(\Delta\eta)^2} + Nb\frac{(\theta_{i+1} - \theta_{i-1})(H_{i+1} - H_{i-1})}{4(\Delta\eta)^2} + Nt\left(\frac{\theta_{i+1} - \theta_{i-1}}{2\Delta\eta}\right)^2 + EcPre^{-\beta\theta_i}\left(\frac{W_{i+1} - W_{i-1}}{2\Delta\eta}\right)^2, \tag{24}$$

$$Sc\frac{dH_i}{dt} = \frac{(H_{i+1} - 2H_i + H_{i-1})}{(\Delta\eta)^2} + \frac{Nt}{Nb}\frac{(\theta_{i+1} - 2\theta_i + \theta_{i-1})}{(\Delta\eta)^2}, \tag{25}$$

with initial conditions

$$\begin{aligned} W = \frac{-fW_2}{\Delta\eta - f}, \theta_2 = \theta_1, H_2 = H_1, w_{N+1} = 1, \\ \theta_{N+1} = \theta_N(1 - Bi\Delta\eta), H_{N+1} = H_N - Nt\frac{(\theta_{N+1} - \theta_N)}{Nb}, \end{aligned} \tag{26}$$

There is only one independent variable in Eqs. (23)-(26), so they are first order ordinary differential equations with known initial conditions. The resulting initial value problem can be easily solved iteratively using Runge-Kutta Fehlberg integration technique implemented on computer using Matlab. From the process of numerical computation, the skin-friction coefficient and the Nusselt number in Eq. (18) are also worked out and their numerical values are presented.

5. Result and discussion

Numerical solution for the representative velocity field, temperature field, nanoparticles concentration and Entropy generation rate have been carried out by assigning some arbitrary chosen specific values to various thermophysical parameters controlling the flow system as presented on the Figs. 2-18. Following Hwang et al. [11] , the Prandtl number (Pr) of the pure water base nanofluid under consideration is assigned the value 6.2.

5.1. Effects of parameter variation on velocity profiles

Figs. 2-5 depict the effects of various physical parameters on the nanofluid velocity profiles. It is noted in Figs. 2 and 5 that as time increases the velocity increases across the channel until it attains a steady state profile for a given set of parameter values. Fig. 4 shows that the nanofluid velocity profile decreases with increasing convective cooling at the walls as the Biot number Bi increases. This may be attributed byNavier slipand increasing rate of heat loss at the channel walls and leading to an increase in the nanofluid thickness and a decrease in the flow speed. It is also observed that the nanofluid velocity decreases with a increase Eckert number Ec, this may bedue to viscous dissipation see Fig. 5. The nanofluid kinetic energy increases with viscous heating; this invariably leads to a decrease in the fluid viscosity and an increase in velocity profile.

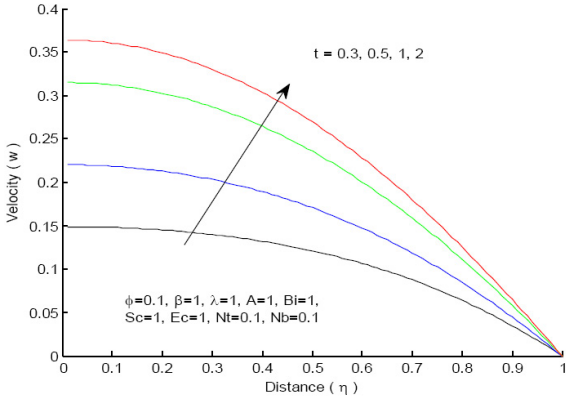

Fig. 2. Velocity profiles across the channel with increasing time.

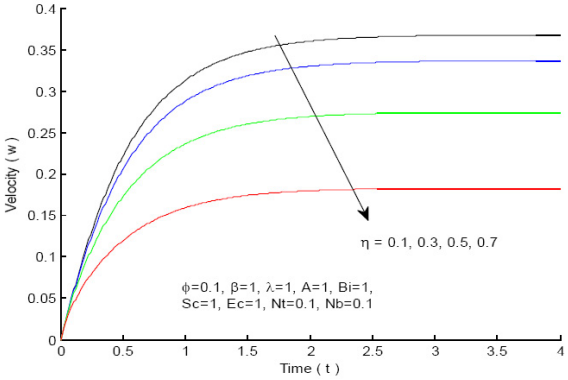

Fig. 3. Velocity profiles with increasing time.

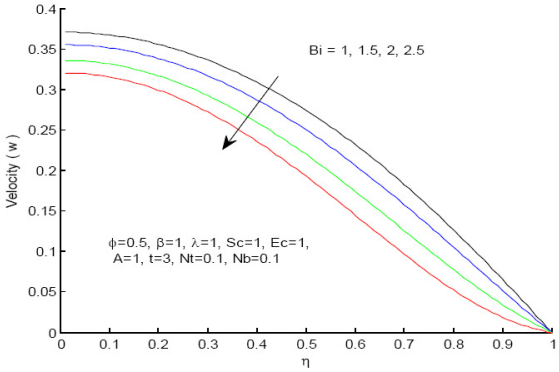

Fig. 4. Velocity profiles with increasing Bi..

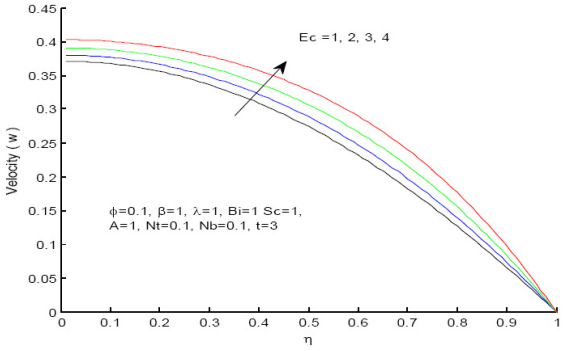

Fig. 5. Velocity profiles with increasing Ec.

5.2. Effects of parameter variation of temperature profiles

Theeffects of unsteadiness and parameter variation on the temperature profiles are illustrated on the Figs. 6-8. In Figs. 6 and 7, we observed the nanofluid temperature decreases across the channel with time and space. The fluid temperature decreases across the channel with increasing convective cooling due to increasing heat loss to the ambient surrounding from the walls. As Biot number Bi increases, consequently, a fall in nanofluid temperature is observed as shown in Fig. 8.

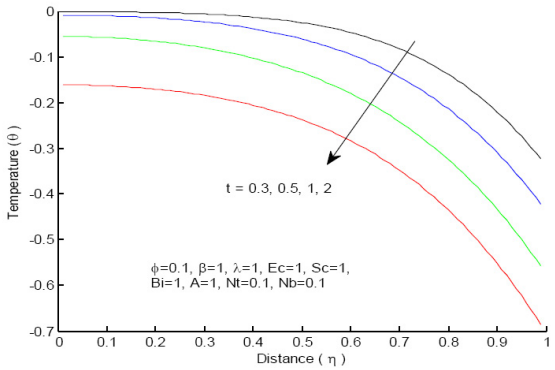

Fig. 6. Temperature profiles with increasing time.

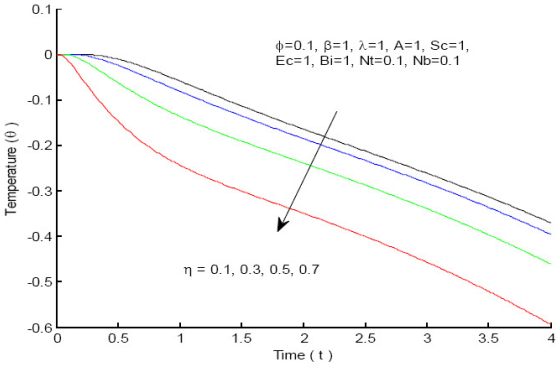

Fig. 7. Temperature profiles with increasing time.

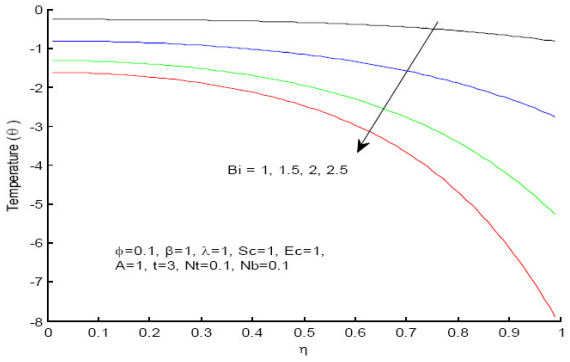

Fig. 8. Temperature profiles with increasing Bi.

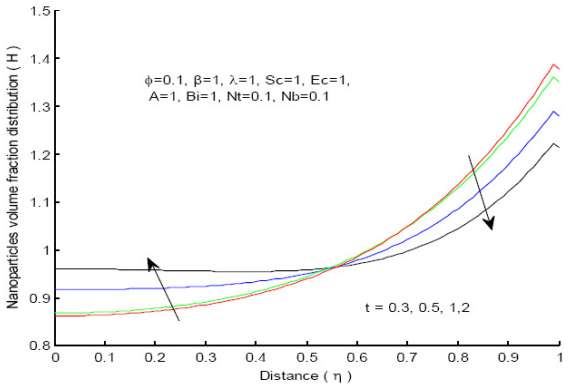

Fig. 9. Nanoparticles distribution with increasing time.

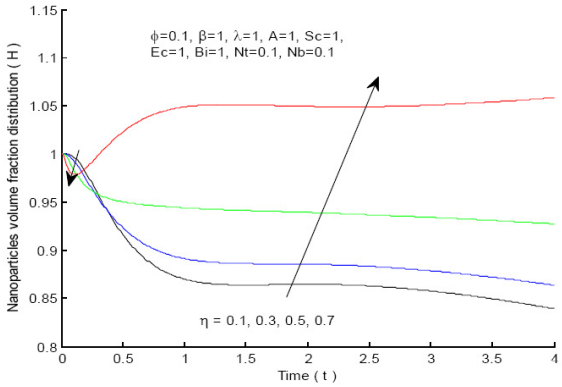

Fig. 10. Nanoparticles distribution with increasing time.

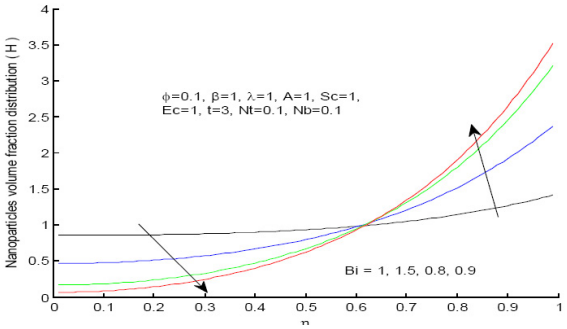

Fig. 11. Nanoparticles distribution with increasing Bi.

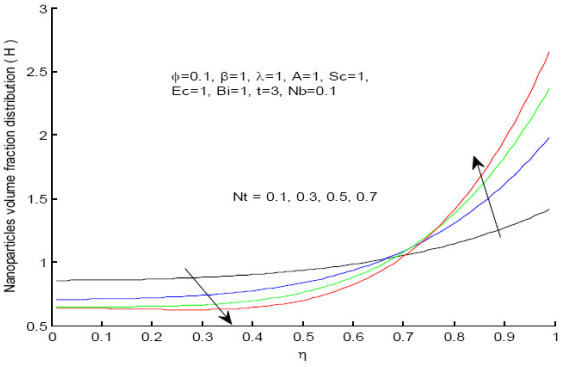

Fig. 12. Nanoparticles distribution with increasing Nt.

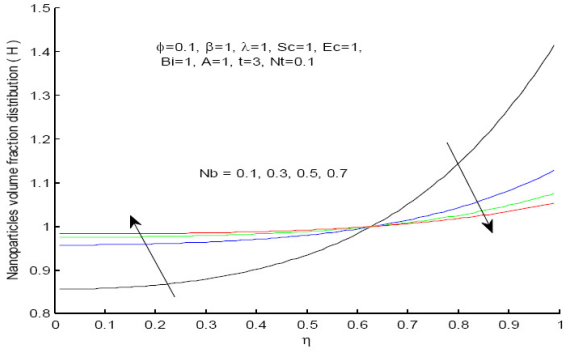

Fig. 13. Nanoparticles distribution with increasing Nb.

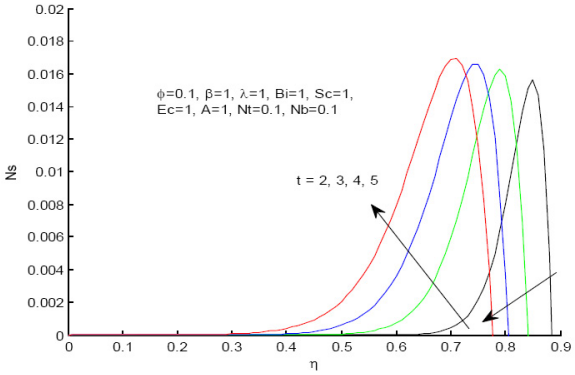

Fig. 14. Entropy generation with increasing time.

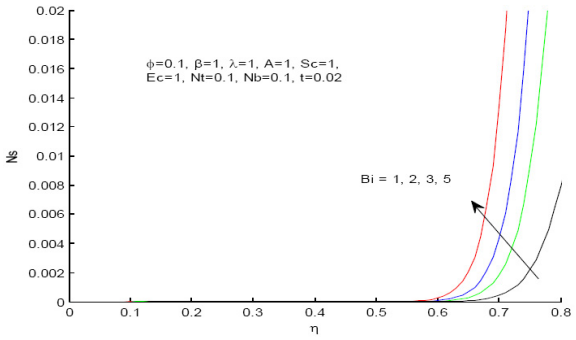

Fig. 15. Entropy generation with increasing Bi.

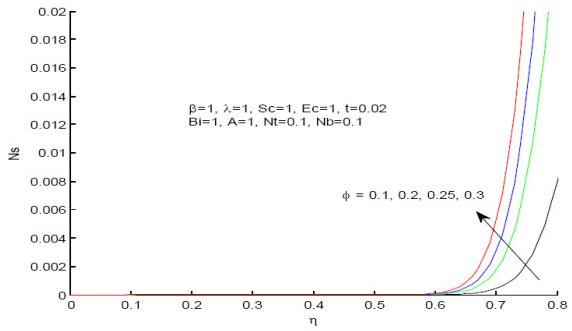

Fig. 16. Entropy generation with increasing ϕ.

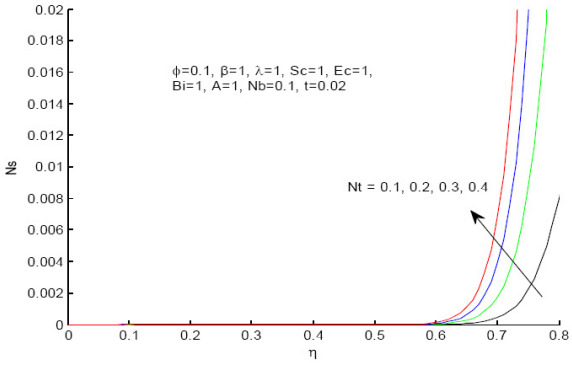

Fig. 17. Entropy generation with increasing Nt.

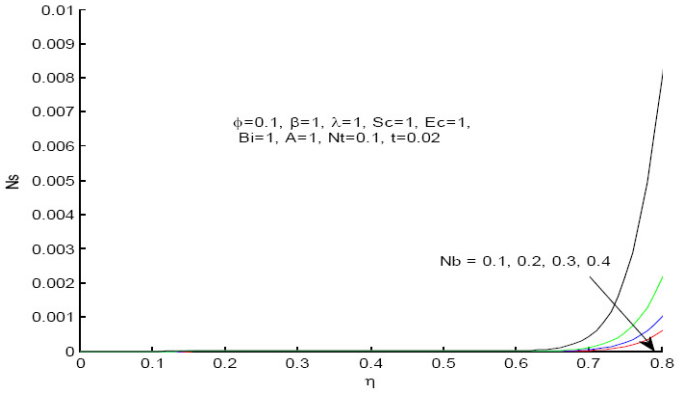

Fig. 18. Entropy generation with increasing Nb.

5.3. Effects of parameter variation on nanoparticles concentration

Figs. 9-13 depict the effects of various physical parameters on the nanoparticles concentration profile. It is observed that the concentration of nanoparticles increases along the channel centreline region $0 \leqslant \eta \leqslant 0.55$ and decreases at the region when $0 \leqslant \eta \leqslant 0.55$ as time increases as shown in Fig. 9. It is also observed that the concentration of nanoparticles increases increase with the increase in space see Fig. 10. Fig. 11 shows a decrease in nanoparticles concentration within the centreline region and decrease in concentration near the lower wall and increase near the upper wall as the Bi increases. This may be attributed to the introduction of Navier slip at the lower wall and kinetic energy of the nanoparticles increases towards the upper wall with a rise in convective heat loss to the ambient. It is observed in Fig. 12 that, with increasing thermophoresis effectNt due to temperature gradient, leading to an increase in nanoparticles concentration at the upper wall and vice-versa at the lower wall. Opposite observation is depicted

when increasing motion of particles (Brownian motion Nb) in a fluid as shown in Fig. 13.

5.4. Effects of parameter variation on entropy generation rate

Figs. 14-18 illustrate the effect of parameter variation on entropy generation rate across the channel. From Fig. 14, it is seen that the entropy generation rate is at steady stat at the interval and start increasing with time as it approaches the upper wall.. This may be attributed by Navier slip at the lower wall and the fact the entropy production depends on velocity, temperature and nanoparticles concentration gradients which vanish along the channel centreline, leading to the minimum entropy generation within this region. Moreover, increase in Biot number lead the entropy generation constant within the channel but increases the entropy generation at the upper wall as shown in Fig. 15. This may be attributed by Navier slip at the lower wall. Similar results are observed in Fig. 16 and Fig. 17 as nanoparticle fraction ϕ and thermophoresis Nt increases respectively. The opposite result is observed in Fig. 18 when increasingmotion of particles (Brownian motion Nb).

6. Conclusions

The flow structure, heat transfer and entropy generation in unsteady channel flow in a variable viscosity transient generalized Couette flow of nanofluids with Navier slip and convective coolingwater based nanofluidswith convective heat exchange with the ambient at the walls are numerically investigated. Using a semi discretization finite difference method together with Runge-Kutta Fehlberg integration scheme, the model nonlinear initial boundary value problem is tackled. Below are some of the results obtained in this study:

- The nanofluid velocity and temperature profiles increase with an increase in time t, Eckert Ec but decreases with an increase in space η and Biot Bi.
- The nanofluid temperature decreases with an increase in time t, space η and Biot Bi.
- The nanoparticles concentration increases at the lower wall and decrease at the upper wall with an increase in time t and motion of particles (Brownian motionNb). Opposite results are observed with an increase in Biot Bi and thermophoresis Nt.
- The constant entropy generation $Ns = 0$ within the channel and increase in entropy generation at the upper wall is observed with increase in Biot Bi, nanoparticle fraction ϕb and thermophoresis Nt. The opposite result is observed when increasing motion of particles (Brownian motion Nb).

Generally, from the above, we conclude that with careful combination of parameter values, the entropy production within the channel flowin a variable viscosity transient generalized Couette flow of nanofluids with Navier slip and convective coolingwater based nanofluids can be minimised.

References

[1] S.U.S. Choi, Enhancing thermal conductivity of fluids with nanoparticles, In: Proc. ASME Int. Mech. Engng. Congress and Exposition, San Franciscos, USA, ASME, FED 231/MD 66 (1995) 99–105.
[2] J. Buongiorno, Convective transport in nanofluids, ASME J. Heat Transfer 128(3) (2006) 240250.
[3] A.V. Kuznetsov, D.A. Nield, Natural convective boundary-layer flow of a nanofluid past a vertical plate, Int. J. Therm. Sci. 49(2) (2010) 243–247.
[4] H.K. Kuiken, An asymptotic solution for large prandtl number free convection, J. Eng. Math. 2(4) (1968) 355–371.
[5] H.K. Kuiken, Free convection at low prandtl numbers, J. Fluid Mech. 37(4) (1969) 785–798.
[6] E. Schmidt, W. Beckmann, Das Temperatur- und Geschwindikeitsfeld von einerwÃd'rmeabgebendensenkrechten Platte beinatÃijrlicherKonvection, II. Die Versuche undihreErgibnisse, Forcsh, Ingenieuscrwes 1 (1930) 391–406.
[7] A. Bejan, Convection Heat Transfer, Wiley, New York, 1984.
[8] A. Mahdy, A. Chamkha, Heat transfer and fluid flow of a non-Newtonian nanofluid over an unsteady contracting cylinder employing BuongiornoâĂŹs model, International Journal of Numerical Methods for Heat & Fluid Flow 25(4) (2015) 703–723
[9] M.H. Mkwizu, O.D. Makinde, Entropy generation ina variable viscosity channel flow of nanofluids with convective cooling, Comptes Rendus Mecanique 343 (2015) 38–56.
[10] M. Shahi, A.H. Mahmoudi, R.A. Honarbakhsh, Entropy generation due to natural convection cooling of a nanofluid, IntCommun Heat Mass Transfer 38(9) (2011) 72–83.

[11] M. S. Alam, M.M. Haque, M.J. Uddin, Convective flow of nanofluid along a permeable stretching/shrinkingwedge with second order slip using Buongiorno's mathematical model, Int. J. Adv. Appl. Math.and Mech. 3(3) (2016) 79–91.
[12] O. D. Makinde, W.A. Khan, Z.H. Khan, Buoyancy effects on MHD stagnation point flow and heat transfer of a nanofluid past a convectively heated stretching/shrinking sheet, International Journal of Heat and Mass Transfer 62 (2013) 526–533.
[13] O.D. Makinde, Computational modelling of nanofluids flow over a convectively heated unsteady stretching sheet, Current Nanoscience, 9 (2013) 673–678.
[14] X. Q. Wang, A. S. Mujumdar, Heat transfer characteristics of nanofluids: a review, Int. J. Thermal Sciences 46 (2007) 1–19.
[15] P.G. Moakher, M. Abbasi, M. Khaki, New analytical solution of MHD fluid flow of fourth gradefluid through the channel with slip condition viacollocation method, Int. J. Adv. Appl. Math. and Mech 2(3) (2015) 87–94.
[16] O.D. Makinde, W.A. Khan, A. Aziz, On inherent irreversibility in Sakiadis flow of nanofluids, International Journal of Exergy 13(2) (2013) 159–174.
[17] D.M. Mwangi, S. Karanja, M. Kimathi, A numerical investigation of the effect of curvature and Reynoldsnumber to radial velocity in a curved porous pipe, Int. J. Adv. Appl. Math. and Mech. 5(1) (2017) 99–110.